A Fully Symmetric and Completely Decoupled MEMS-SOI Gyroscope

A. Sharaf [1,2], S. Sedky[2], M. Serry[3], A. Elshurafa[3], M. Ashour[1] and S. E.-D. Habib[4]

[1]Egyptian Atomic Energy Authority, Cairo, Egypt
[2]American University in Cairo, Cairo, Egypt
[3]King Abdullah University of Science and Technology, Thuwal, Saudi Arabia
[4]Electronics and Communications Dept., Faculty of Engineering, Cairo University, Egypt

ABSTRACT

This paper introduces a novel MEMS gyroscope that is capable, for the first time, of exciting the drive mode differentially or in common mode. The structure also decouples the drive and sense modes via an intermediate mass and decoupling beams. Both drive and sense modes are fully differential enabling control over the zero-rate-output for the former and maximizing output sensitivity using a bridge circuit for the latter. Further, the structure is fully symmetric about the *x*- and *y*- axes. Complete analytical analysis based on the equation of motion was performed and verified using two commercially available finite element software packages. Results from both methods exhibit good agreement. The analysis of the sensor shows an electrical sensitivity of 1.14 (mV/ (°/s)).

Keywords: Gyroscopes, MEMS, Silicon-on-Insulator (SOI), Mechanical sensitivity.

1 INRODUCTION

Conventional rotating wheel gyroscopes and optical gyroscopes are bulky and expensive to be used in most modern applications. Micromachining, on the other hand, can shrink both size and weight of the sensor by orders of magnitude, reduce the fabrication cost significantly, and allow the electronics to be integrated on the same silicon chip. Thus, MEMS-based gyroscopes and MEMS inertial sensors in general have received particular attention in the last decade.

Despite the several advantages attained from MEMS gyroscopes, their performance is still unacceptable for applications that require tactical- and inertial-grade performance. Most of current micromachined gyroscopes that are implemented in most automotive applications today require rate-grade performance [1]. Achieving tactical- and inertial-grade performance is challenging as it implies significant mechanical and electrical design tradeoffs. Several researchers are trying to overcome this limitation [2-8]. This paper takes a step in proposing a possible solution that could achieve inertial-grade performance and further, introduces several enhancements to the design of MEMS gyroscopes in general.

Section 2 presents the design of the gyroscope and explains its new features. Then, Section 3 includes the theoretical analysis. Section 4 summarizes the results acquired from the finite element software packages before verifying them with measurements in Section 5. Finally, the paper is concluded in Section 5.

2 GYROSCOPE DESIGN

In this work, a novel fully symmetric and completely decoupled MEMS gyroscope (FSCDMG) is presented as shown in figures 1- a, b.

The proposed structure is designed according to the principle of decoupling the drive and sense modes [10]. The structure is fully symmetric about *x*- and *y*- axes, and complete decoupling is achieved by separating the drive and sense elements via the intermediate mass and the decoupling beams. The gyroscope thickness is 5 µm, and the minimum features for gap spacing, spring width, and comb drive width are 2 µm. If the sensor is fabricated by deep reactive ion etching (DRIE) process, a significant increase in the sensor performance can be achieved easily. This design alleviates most of the micromachined gyroscope drawbacks such as asymmetry and coupling. Furthermore, it allows actuating the sensor with higher electrostatic force, and increases the sense capacitance.

The design under consideration enables exciting primary mode oscillations along the *x*-axis in either differential or common mode. In addition, the amplitude of the drive mode vibration is kept constant all the time using a sense and feedback control system connected to the drive mass. Also four sets of control combs are used to tune the resonance frequency externally via electric voltage. Using the intermediate mass and decoupling beams, complete decoupling is achieved. The second part of the sensor is the intermediate mass, which has two degrees of freedom; this mass is designed to decouple the primary and secondary mode oscillations to minimize the mechanical crosstalk. The sense mass consists of two identical sense elements each of which carries two sense capacitors. These capacitors are connected differentially to cancel any interference of the drive mode motion into the output signal.

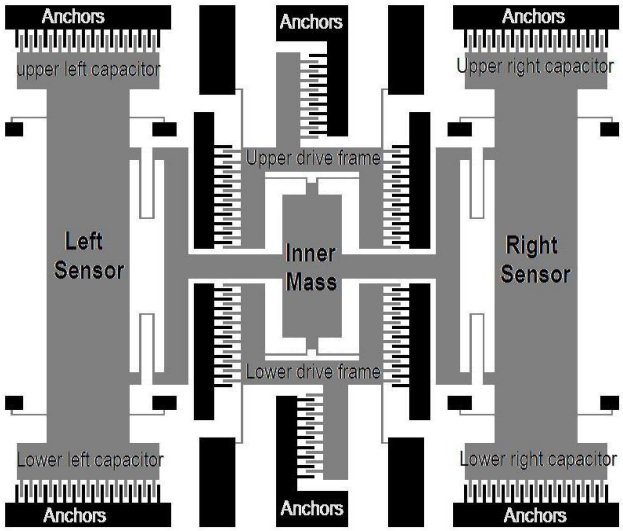

Figure 1-a: Simplified Schematic diagram of the designed sensor

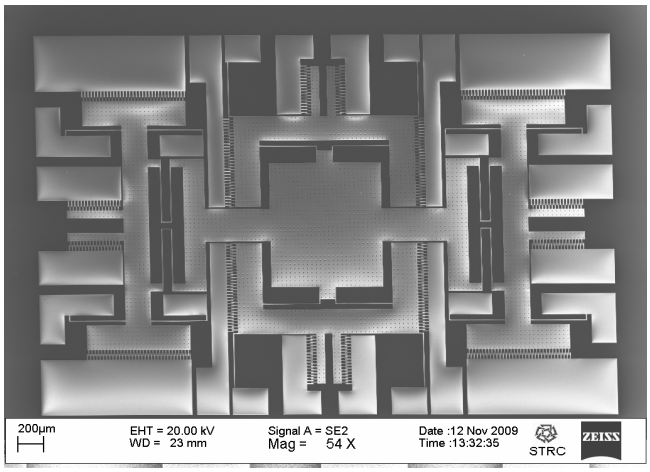

Figure 1-b: SEM image of the fabricated gyroscope.

3 ANLYSIS

3.1 Analytical Analysis

Two C-shaped frames are arranged to consist the drive mass as shown in fig. 1. They are attached to the substrate via four crab-leg beams, and to the intermediate mass via another four crab-leg beams. The drive mass carries four sets of comb drive assemblies to provide the required driving electrostatic force. The drive mass is designed to have only one degree of freedom along the *x*-direction (i.e. drive mode). These four sets of comb drive actuators are used to produce the required exciting electrostatic force. The actuators are organized in such a way that provides either differential or common mode actuation.

The sense element is divided into two identical sense masses. Each mass carries sets of comb drive capacitors. Each half of the sets is composed of one capacitor, and these capacitors are connected differentially to suppress any off-axis displacement

Based on the equation-of-motion-analysis [4], the mechanical sensitivity is given as:

$$S_m = \left|\frac{y}{\Omega}\right| = \frac{2m\omega_x Q_x Q_y F_d}{K_x K_y}$$

Connecting the sense capacitors differentially, the output voltage at the center of the divider is at the frequency of the carrier signal, and has amplitude of [4]:

$$V_o = \frac{C_2}{C_1 + C_2} V_m = \frac{V_m}{2} + \frac{y.V_m}{2.l_o}$$

Typical values of l_o and g_o are 20 µm and 2 µm respectively.

3.2 Numerical Analysis

Finite element analysis is used to determine the natural frequency and the load characteristics of the sensor. The commercially available software packages ANSYS and COMSOL are used to verify the analytical model.

4 RESULTS

The analytical results (ANA) based on the equations of motion [4] are summarized in Table 1. The resonance frequencies are 16,814 Hz and 16,816 Hz for drive and sense modes respectively, which indicate a high matching operation condition that allows amplifying the sense mode displacement by the sense mode quality factor.

Finite element analysis has been performed using ANSYS (FEM1) and COMSOL (FEM2). Modal analysis was used to extract the mode shapes and natural frequencies of the structure. Fig. 2 shows the drive mode shape at a resonance frequency (F_x) of 16,769 Hz according to COMSOL. The dashed lines in the figure represent the unexcited structure and indicate that this mode shape is translational as desired. Similarly, Fig. 3 shows the second mode shape (sense mode) at a resonance frequency (F_y) of 16,797 Hz.

Harmonic analysis was also performed to examine the response of the structure to dynamic loads. Figure 4 shows the frequency response of the drive mode when the structure is loaded with and input rotation rate of 1°/s. Fig. 4 shows drive mode amplitude (X_d) of 17.56 µm, and Fig. 5 shows the frequency response of the sense element. It shows a large output displacement (Y_s) of 0.351 µm. Table 2 summarize these results and compares with one of the most successful symmetric and decoupled gyroscope designs [2]. The mechanical sensitivity (S_m) and the electrical sensitivity (S_e) of the sensor are 0.005 µm/ (°/s) and 1.14 mV/ (°/s) respectively.

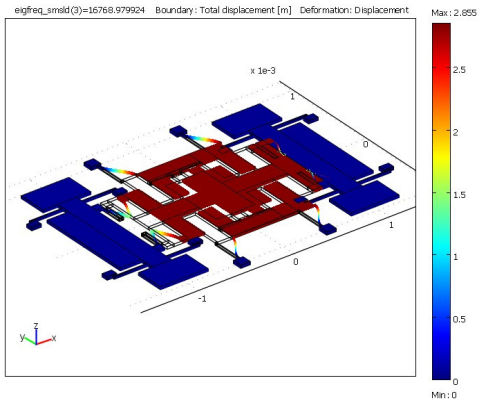

Figure 2: Drive mode shape (16,769 Hz)

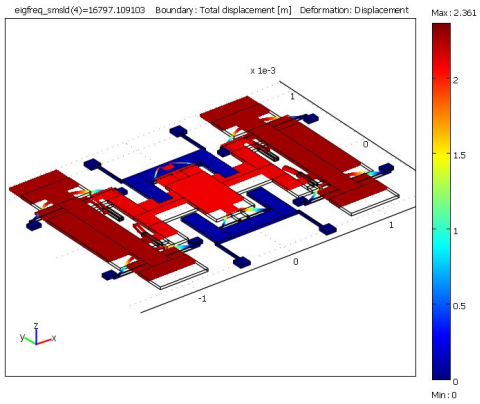

Figure 3: Sense mode shape (16,797 Hz)

TABLE 1
ANALYTICAL VS. NUMERICAL RESULTS FOR THE FSCDMG.

	Results			% mismatch		
	ANA.	**FEM1**	**FEM2**	**ANA Vs FEM1**	**ANA Vs FEM2**	**FEM1 Vs FEM2**
F_x *(Hz)*	16814	16786	16769	0.17	0.27	0.1
F_y *(Hz)*	16816	16800	16797	0.1	0.11	0.02
% mismatch	0.01	0.08	0.17	---	---	---
X_d *(µm)*	14	17.56	17.28	20.27	18.98	1.59
Y_s *(µm)*	0.52	0.351	0.342	32.5	34.2	2.56
S_m *(µm/(°/s))*	0.005	0.003	0.003	-----	----	----
S_e *(mV/(°/s))*	1.14	0.684	0.679	-----	----	----

5 EXPERMENTAL RESULTS

The FSCDMG was fabricated using single mask on a silicon-on-insulator (SOI) wafer to define the structure, and the subsequent release was performed using HF wet etching. The Agilent 4395A Network/Spectrum analyzer is used to characterize the resonance frequency of the sensor. The test setup is shown in Fig. 6 and the measured resonance frequencies for the drive and sense modes were found to be 18,045 Hz, 17,950 Hz respectively as shown in figs. 7 and 8 respectively. It was found that the quality factor of ~10 which is very low because the measurements are being performed in ambient pressure.

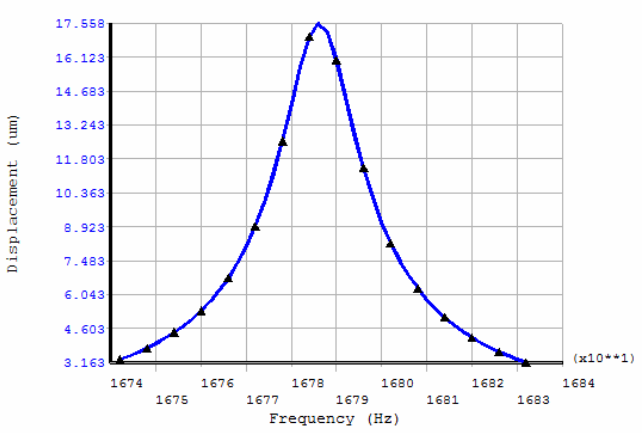

Figure 4: Frequency response of the drive mode

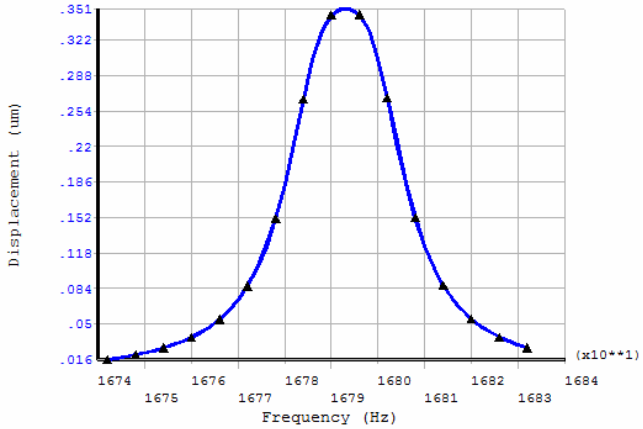

Figure 5: Frequency response of the sense mode.

TABLE 2
COMPARISON BETWEEN FSCDMG AND SYMMETRIC DECOUPLED GYRO OF REF. [2] .

Parameter	**Results**		
	FSCDMG (Simulated)	*Ref. [2] Gyro (Simulated)*	*Ref. [2] Gyro (Measured)*
Area (mm^2)	1.6 × 1.6	2.9 × 2.9	2.9 × 2.9
Drive capacitance	239 fF	352 fF	405 fF
Sense Capacitance	274.5 fF	381 fF	455 fF
Drive mode freq. (Hz)	16786	4678	4090
Sense mode freq. (Hz)	16800	4823	4363
Freq. mismatch (%)	0.08	3.01	6.3
Drive amplitude (µm)	17.56	------	10
Sense amplitude (nm)	0.351	0.61	------
Mechanical sens. (µm/°/s)	0.003	-----	-----
Electrical sens. (mV/°/s)	0.684	0.280	0.180
Drive mode quality factor	933	-----	900 (vacuum)
Sense mode quality factor	840	-----	550 (vacuum)
Measurement range (°/s)	±150	± 100	-----
Scale Factor (mV/°/s)	-----	----	17.7

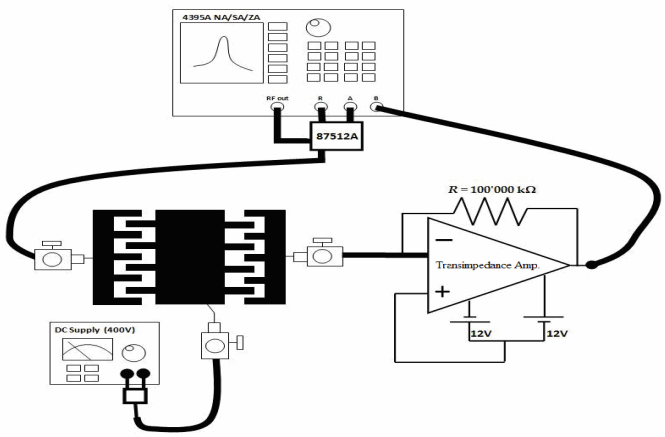

Figure 6: Schematic diagram shows the resonance frequency measurement.

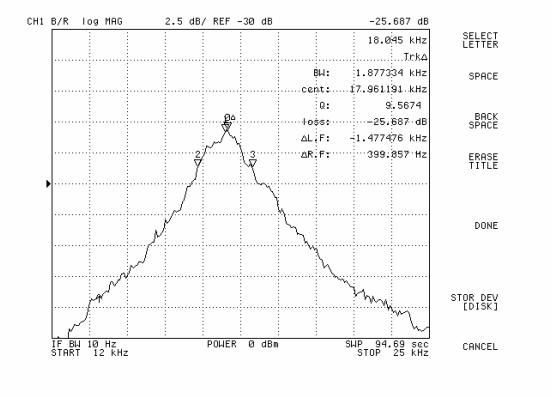

Figure 7: Drive mode resonance frequency measurement

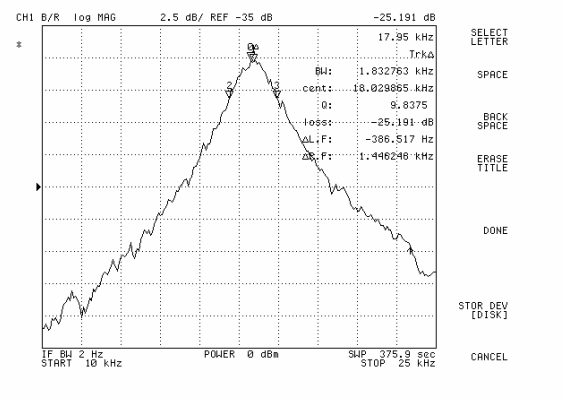

Figure 8: Sense mode resonance frequency measurement

6 CONCLUSION

This work introduces a new structure for symmetric and decoupled vibratory MEMS-SOI gyroscopes possessing three masses. The design under consideration enables exciting primary mode oscillations along the *x*-axis in either differential or common mode schemes. The output signal is sensed by two identical sense element capacitors, which are connected differentially to cancel any interference of the drive mode motion into the output signal. The sensor performance is enhanced significantly by operating it in matched mode.

REFERENCES

[1] N. Yazdi, et.al., "Micromachined Inertial Sensors," in the proceeding of the IEEE, Vol. 86, No. 8, PP. 1640-1659, August 1998.

[2] S. E. Alper, et.al., "A low-cost rate-grade nickel microgyroscope," Sensors and Actuators A, Vol. 132, PP. 171-181, 2006.

[3] J. Kim, et.al., "Robust SOI process without footing and its application to ultra high-performance microgyroscopes," Sensors and Actuators A, Vol. 114, PP. 236-243, 2004.

[4] Abdelhameed Sharaf, Sherif Sedky and S. E.-D. Habib, "Complete analysis of a novel fully symmetric decoupled micromachined gyroscope," the 2006 international conference on MEMS, Nano and Smart systems, PP. 35-40, 27-29 Dec. 2006.

[5] W. Geiger, et.al., " The silicon angular rate sensor system MARS-RR," Technological Digest, in: Proceedings of the 10th International Conference on Solid-State Sensors and Actuators (Transducers'99), Sendia, Japan, PP. 1578-1581, 7-10 June, 1999.

[6] K. Maenaka, et.al., "MEMS gyroscope with double gimbal structure," in: Proc. of the 12th Inter. Conference on Solid-State Sensors, Actuators and Microsystems (Transducers'03), Boston, PP. 163-166, 2003.

[7] S. E. Alper and T. Akin, "A single-crystal silicon symmetrical and decoupled gyroscope on insulating substrate," in: Proceeding of the 12th International Conference on Solid-State Sensors, Actuators and Microsystems (Transducers'03), Boston, PP. 1399-1402, 2003.

[8] Huihai Xie and Gary Fedder, "Integrated microelectromechanical gyroscopes," Journal of aerospace engineering, ASCE, PP. 65-75, April, 2003.

[9] Hazusuke Maenaka, et.al, "Design, Fabrication and Operation of MEMS Gimbal Gyroscope," Sensors and Actuators A, V 121, PP. 6-15, 2006.

[10] W. Geiger, et.al., "Decoupled microgyros and the design principle DAVED," Sensors and Actuators A, Vol. 95, PP. 239-249, 2002.